

Crustal Thickness Variation in the Andean Foreland, Argentina, from Converted Waves

by Marc Regnier, Jer-Ming Chiu, Robert Smalley, Jr., Bryan L. Isacks, and Mario Araujo

Abstract Local network three-component digital data from the San Juan area, Argentina, provide the first seismological images of the deep crustal structure in the Andean foreland above a horizontal segment of the subducted Nazca plate. We have identified *S*-to-*P* seismic phases converted on the Moho by analysis of seismograms formed by taking the product of the radial and vertical components ($R * Z$) from intermediate-depth earthquakes in the Benioff zone directly beneath the network. Under the Sierras Pampeanas, the Moho is estimated to be at a depth of about 52 km. Beneath the eastern Precordillera, the Moho deepens to 55/57 km and further west, beneath the central Precordillera, to 60 km. We therefore estimate a 5° to 10° westward dip to the Moho under the Andean foreland. In both the Sierras Pampeanas and Precordillera provinces, the thickness of the ductile lower crust is comparable to that for a stable continental crust, while the brittle upper crust, implied from the spatial distribution of the seismicity, shows an important thickness increase. This rheological behavior is interpreted to be a consequence of the flattening of the dip of the subducted plate. The east–west deepening of the seismicity, the Moho, and the depth to basement under the Precordillera all suggest that the Andean foreland lithosphere is underthrusting beneath the Andes. The associated shortening is estimated to be about 15% across the Sierras Pampeanas. It is estimated to be at least 38% across the Precordillera for the part of the crust beneath the décollement, while it is up to 70% for the part above the décollement.

Introduction

Recently, several articles have dealt with kinematic evolution of the Andean orogen (Isacks, 1988; Allmendinger *et al.*, 1990; Sheffels, 1990), and they have shown that models involving a large amount of crustal shortening could satisfactorily explain the main morphotectonic features of the Andes. In an attempt to quantify this amount of shortening across the entire Andean orogenic belt at 30° S latitude, Allmendinger *et al.* (1990) proposed a family of models that can account for the uplift of the high Cordillera but differ in the manner that they link upper and lower crustal deformation. A key parameter of these models to further constrain the mode of deformation in the lower crust is the crustal thickness. Indeed, knowing the upper crustal structure and the depth extent of the brittle deformation, the determination of the Moho depth should allow us to better estimate the amount of ductile thickening in the lower crust. To date, very few measures of crustal thickness have been obtained in South America, and especially in the Andes. To provide such important information, a portable seismic network (PANDA, Chiu *et al.*, 1991) was operated in the prov-

ince of San Juan, Argentina, (Figs. 1 and 2) from August 1987 to May 1988. The network was located above a subhorizontal subducting segment of the Nazca plate. The numerous intermediate-depth earthquakes from the Wadati–Benioff zone (Fig. 3) recorded by the whole network provide an opportunity to study the crustal structure of the Andean foreland and Precordillera thrust belt through sampling by upgoing ray paths. In this area, the foreland is a distinctive morphotectonic province characterized by a series of mountains and basins, the Sierras Pampeanas. Although the Sierras Pampeanas are not part of the morphological Andes, they are an integral part of the Andean deformation, and shortening in that province is important to the overall estimation of crustal shortening. The Precordillera is the easternmost belt of the Andes and its relationship to the Sierras Pampeanas is not well understood, especially at depth where there are very few structural constraints. The amount of crustal thickening, however, can be estimated from the crustal thickness beneath seismic stations, as determined from travel-time analysis of Moho converted waves from un-

derlying intermediate-depth events (Fig. 3). Significant amounts of crustal thickening can then be related to shortening of the total crust under the Sierras Pampeanas and the Precordillera.

Regional Setting

The Sierras Pampeanas, a region of Precambrian metamorphic basement block uplifts (Caminos *et al.*, 1982), is the easternmost province of the Andean orogen between 28° and 33° S (Fig. 1). These ranges are east of and adjacent to the Precordillera, a narrow foreland

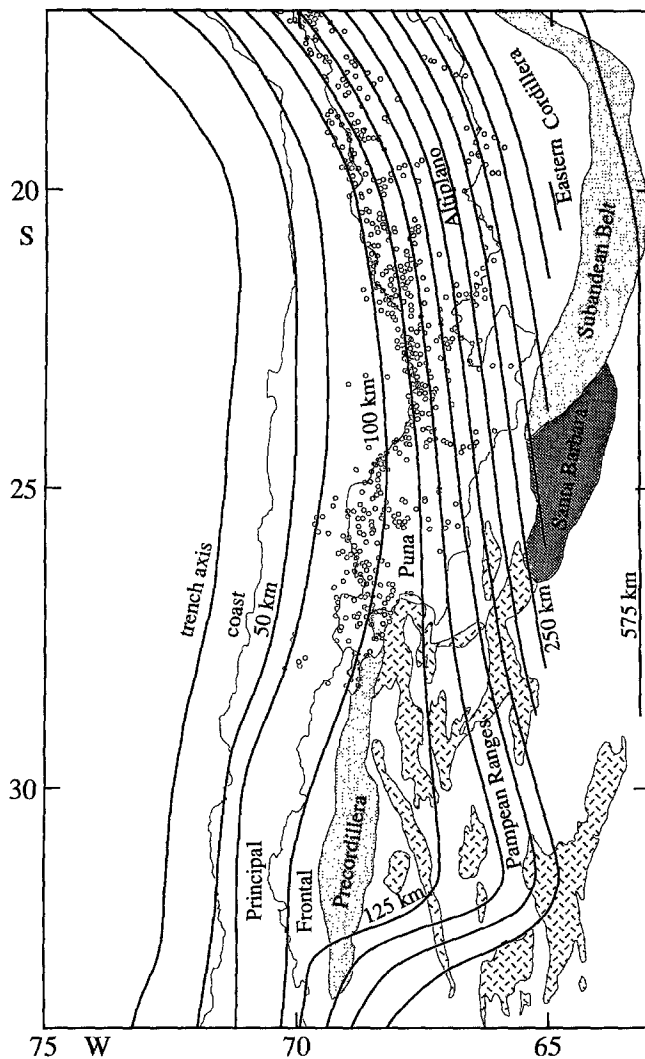


Figure 1. Map of western South America illustrating upper plate tectonic features, volcanic arc, and contours of the Wadati-Benioff zone (WBZ). Along-strike segmentation of the upper plate tectonic provinces correlates with the along-strike segmentation of the WBZ (Jordan *et al.*, 1983). The distribution of Neogene volcanos (open circles) (Isacks, 1988) shows an active magmatic arc over the steep WBZ segment and the absence of an active arc over the flat segment.

thrust belt which ends eastward the physiographic Andes (Fig. 1). Such thick-skinned deformation east of the thin-skinned thrust belt is unusual and found only in regions overlying subhorizontal subduction (Dickenson and Snyder, 1978). Both provinces have a bimodal depth distribution of seismicity corresponding to intermediate-depth events of the subhorizontal Wadati-Benioff zone of the subducted Nazca plate and the crustal events located in the upper plate (Fig. 3). The Sierras Pampeanas mountains are bounded by moderately dipping thrust faults whose seismic activity extends down to a maximum depth of 30 km (Kadinsky-Cade and Reilinger, 1985; Smalley and Isacks, 1990; Regnier *et al.*, 1992). In the Precordillera, the seismicity is confined to the basement at depth between 5 and 35 km in a pattern of segmented faults that do not correlate with the surface mapped faults (Smalley *et al.*, 1993). Ongoing deformations started 10 m.y. ago in the central Precordillera and spread eastward to affect the eastern Precordillera 2.3 m.y. ago (Johnson *et al.*, 1984; Whitney *et al.*, 1984; Bastias *et al.*, 1984). Thrusting in the Sierras Pampeanas is estimated to be younger than 10 m.y. and coincident with the shut-down of the volcanic arc in this segment of the Andes (Kay *et al.*, 1988).

Data and Method

Crustal and upper mantle velocity structures have been successfully investigated using converted waves at interfaces beneath seismic stations at both short (Smith, 1970; Chiu *et al.*, 1986; Li *et al.*, 1992) and teleseismic epicentral distances (Bath and Stefansson, 1966; Jordan and Frazer, 1975; Langston, 1979). In particular, converted phases are extremely useful to determine the velocity and geometry of deep structures that cannot be imaged easily with seismic refraction or reflection profiles. At short epicentral distance, because of the large *S*-wave amplitude, the most pronounced converted phase is often the *S*-to-*P* phase (*Sp*), and both its relative travel times *T* (*S*-*Sp*) and amplitudes can be used to constrain the velocity model where the conversions occurred. In this study, we used transmitted *Sp* converted waves from intermediate-depth earthquakes in the subhorizontal Wadati-Benioff zone and recorded by a local network of three-component seismic stations. The network was operated in the San Juan area from September 1987 to May 1988 and covered an area of roughly 150 km north-south by 100 km east-west (Fig. 2). The network consisted of 26 sites, three of which (CFA, LFL, and LLA) contained small-aperture (several meters to 1 km) multi-station arrays (six to 11 three-component stations). Our study uses a subset of about 300 A quality events (events with well-recorded arrivals through the whole network) during a period when the complete network was operational. The phase reading procedure was identical to that described in Regnier *et al.* (1992). Initial locations were

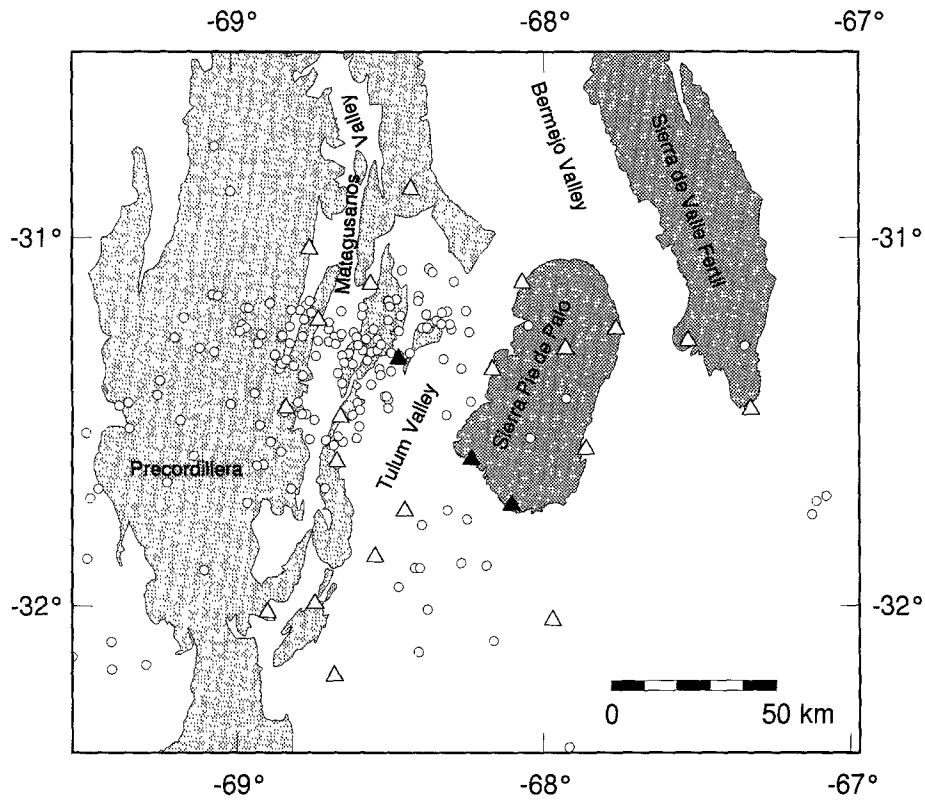


Figure 2. Map of San Juan region. Mountain ranges are shaded light for the sedimentary rocks of the thin-skinned Precordillera and dark for the basement block uplifts of the Sierras Pampeanas. Intermontane valleys of Carboniferous to Quaternary sediments are shown in white. The eastern Precordillera is the chain of mountains east of the Matagusanos Valley. The seismic network stations are shown by open triangles for the three-component high-gain/low-gain stations and solid triangles for the small-aperture arrays composed of multiple three-component high-gain/low-gain or high-gain/high-gain stations. Intermediate-depth epicenters (JHD locations) used in this study are also shown.

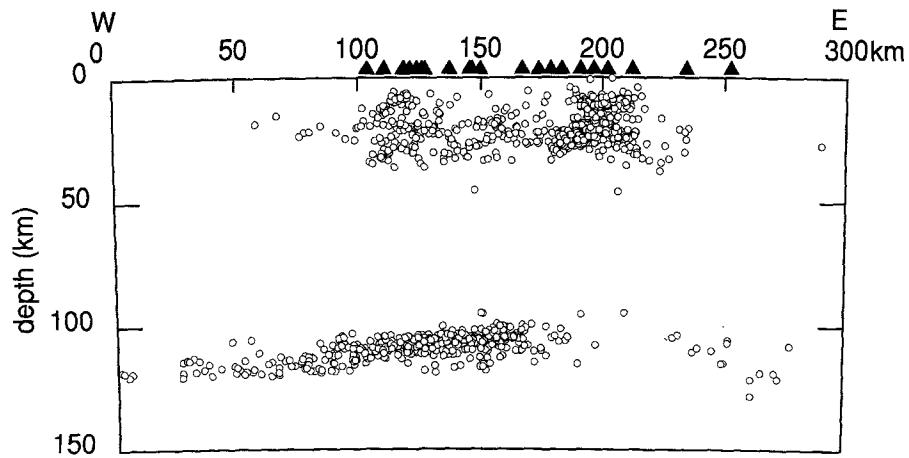


Figure 3. Selected shallow- and intermediate-depth earthquakes from the San Juan region. The east-west cross section shows seismicity has bimodal depth distribution (crustal and WBZ). Crustal seismicity is associated with the Pampean range Sierra Pie de Palo and the eastern side of the Precordillera. Projection of the locations of the PANDA stations are indicated by the solid triangles.

obtained using HYPOINVERSE (Klein, 1978) and a three-layer velocity model (Table 1) modified from the four-layer model of Bollinger and Langer (1988). Both P and S arrivals were used for locating the earthquakes with a V_p/V_s of 1.75, which was obtained from a least-squares fit of a line on Wadati diagrams (Vlasity, 1988). Average rms residuals of approximately 0.3 sec were found for our three-layer velocity model, or slight variations of it. Final locations were obtained using joint hypocentral determination, JHD, (Frohlich, 1979), which reduced the average rms residual of the data set to 0.2 sec. Finally, over 90% of the locations have estimates of epicentral and depth errors of 1 km and 2 km, respectively.

Figure 4 shows an example of an intermediate-depth earthquake recorded at one station of the network. The data suggests arrivals of energy on the Z component between the P and S arrivals but it is not possible to unambiguously identify and pick the corresponding phase in the raw data, as it is mixed with scattered energy. To enhance body-wave phases that are coherent on two of the three directions Z , R , and T , the products $R * Z$ and $T * Z$ are computed. Important properties of the RZ product, pointed out by Jacob and Booth (1977), are that waves with elliptical particle motion are attenuated and coherent rectilinear motion is enhanced. In addition, P and S wave types have opposite signs; for P the RZ product is positive, while for S the RZ product is negative. Because of the high-frequency content of the body waves, the products were computed with the raw data. Low-pass filtering of the data prior to the product resulted, in most cases, in a loss of efficiency of the product operation. Since we did not use amplitudes, the computed products have then been low-pass filtered below 5 Hz to be more easily interpreted. On the RZ product (Fig. 4), it is now possible to identify clear P -type arrivals between the P and S , which we interpret as S -to- P (Sp) converted waves at discontinuities beneath the network. The first large amplitude in the Sp wave group is interpreted to be the S -to- P conversion from the Moho. The coda of this arrival, mainly composed of successive Sp phases, indicates that the crust is highly layered and/or fractured. As we are dealing with three-component data, we also

compute the TZ product. The two products show that body-wave energy, in both the direct P and secondary phase, is usually split between the three directions of motion, indicating waves have propagated through a complex 3D velocity structure (Langston, 1977). However, we did not observe secondary arrivals systematically at any station. No dependence of the presence of the Sp phase with distance or backazimuth could be established. The occurrence of the Sp phase is more likely due to a favorable coupling of adequate focal mechanism and local focusing effect at the base of the crust. Considering the small seismic wavelength used in this study, between 0.5 and 1 km, it is not surprising to observe important variation in the Sp amplitude.

Sierra Pie de Palo

The record section of Figure 5 presents the $R * Z$ product for many earthquakes recorded across the sub-network located on the Sierra Pie de Palo. To remove the source depth effect when searching for the Sp phase, traces are lined up on the S arrivals. They are also cut before the S arrival because the RZ product of that phase is so large that it dramatically scales down any smaller signal when displayed. One can see large arrivals of energy between the P and S phase. From its polarity and apparent phase velocity across the array, we interpret this body wave to be the S -to- P converted wave from the Moho. Theoretical arrival times curves for S and Moho S -to- P conversion are also shown. They are calculated using the same velocity model (Bollinger and Langer, 1988) used for the locations but with a 50-km-deep Moho instead of the initial 45-km depth. The velocities of the model have not been changed.

For each station, a least-square solution of the depth of a horizontal Moho was estimated, minimizing the residues of the relative S - Sp time for a varying Moho depth. The S - Sp relative times were modeled using the velocity model of Bollinger and Langer (1988) and allowing only the Moho depth to vary. The top layers of the Bollinger and Langer velocity model were derived from shallow refraction surveys in the San Juan area (YPF, unpublished data) and most of our stations were on outcrops of Precambrian metamorphic crystalline rock or competent sedimentary rock. We therefore consider that we have a good control on the upper crustal structure beneath the stations and that it would not be appropriate to constrain some of the upper crust parameters further with our data. The major source of error comes from picking the Sp phase. Even on the products, it can be slightly emergent and we estimate the uncertainty in picking the arrival time of the Sp phase to be 0.2 sec. The uncertainty from earthquake location is one order less and will not seriously affect our Moho depth determination since the S - Sp time does not vary significantly over the range defined by the errors on earthquake depth and distance.

Table 1
Crustal Velocity Models*

Three Layers over Half-Space Model	
Depth (km)	Velocity (km/sec)
0.0	5.88
10.0	6.20
32.0	7.30
45.0	8.10

*Three-layer model used in San Juan area; the top layer of the velocity model is based on shallow refraction data (Bollinger and Langer, 1988) and the bottom two layers from regional earthquake studies (Volponi, 1968).

Another possible source of error on the Moho depth determination can be noticed if one looks at the geometry of ray paths used in this study. Figure 6 represents a cross section with two intermediate-depth earthquakes at different epicentral distances together with the ray paths of all the direct waves generated in a two-layer velocity model. First, one can see that at a given distance the P_s and Sp phase do not convert at the same place on the interface. The main feature is the large moveout of the conversion point of the Sp phase with distance, while the conversion point of the P_s remains pretty much below the station (see inset in Fig. 6). This large variation spreads the sampling of the Moho over a wide area and introduces scatter due to both azimuthal and distance dependent variation in Moho depth. Since we are using short-period data, it is also likely that a "minimum noise" is present in the Moho depth measurements due to short wavelength topographic variations of the Moho. In order to reduce the effect of distance dependent variation of the Moho depth, we have only used events with epicentral distance to each individual station less than 50 km. Figure 7 displays an example of rms curve as a function of Moho depth for the station i15. As expected, for a given crustal velocity model, one can see a strong dependence on Moho depth. For the Pie de Palo subnetwork, the rms are generally inferior to 0.3 sec with an

average of 0.2 sec, roughly corresponding to an error of ± 2 km on the Moho depth determination. Figure 8 shows a map with Moho depths determined at a single station. The depth beneath Pie de Palo ranges from 48 to 55 km. A systematic increase in Moho depth is observable from south to north with an average Moho depth of 50 km and 53 km in the southern and northern parts of the sierra, respectively. This result is in agreement with the tectonic model proposed by Regnier *et al.* (1992) of a range divided in two blocks.

To confirm these average Moho depths, we have looked at Sp phases from intermediate-depth earthquakes located beneath the Sierra de la Valle Fertil and recorded at the western stations of the network. Figure 9 shows a record section for Precordillera stations of RZ products. For each trace, backazimuth is roughly eastward. The distance is large enough so the S -to- P conversion point lies beneath the Sierra Pie de Palo (see Fig. 6). Theoretical arrival times for S and S -to- P conversions from a 50-km-deep Moho are also shown. The onset of coherent arrival of energy between the P and S line up well along the S -to- P curve. This result agrees with the Moho depth determined at stations located on the sierra using underneath intermediate-depth earthquakes.

The average crustal thickness of 52 km found beneath the Sierra Pie de Palo is greater than the average

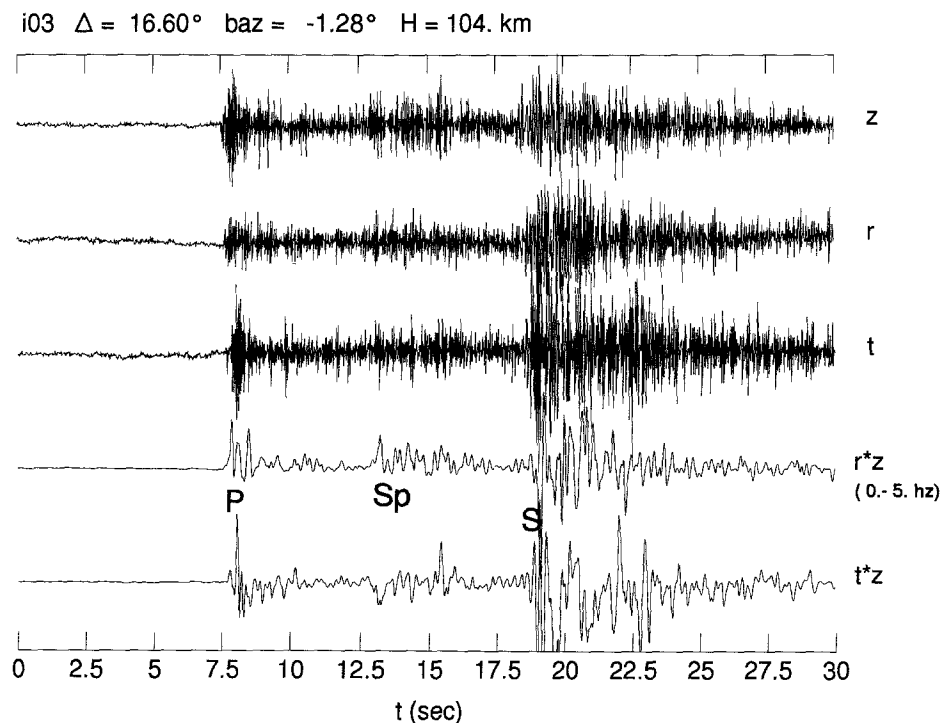


Figure 4. Example of an intermediate-depth earthquake recorded at one station on the Sierra Pie de Palo. The three-component data are normalized together. There are suggestions on the raw data of arrivals of energy between the P and S arrivals. The Sp phase is clearly revealed by the RZ product. Both products are low-pass filtered for easier interpretation. Energy in the TZ product indicates a complex 3D velocity structure.

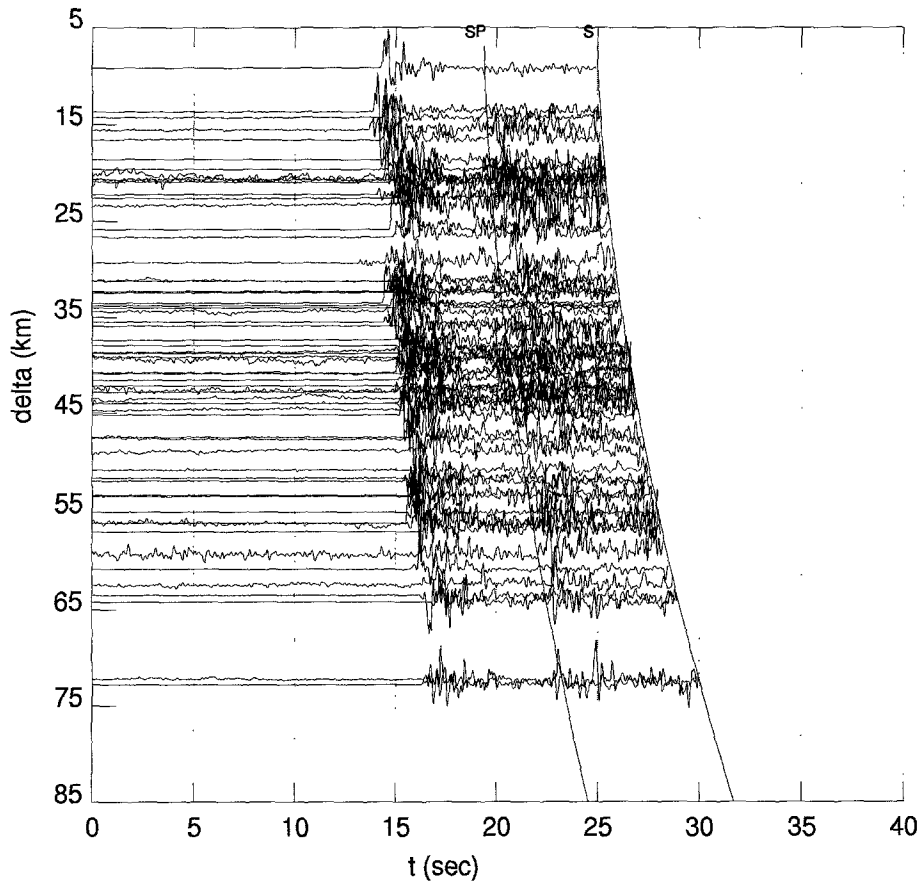


Figure 5. Multiple stations/many earthquakes *RZ* product record section that clearly shows coherent arrival of energy between *P* and *S* phases across the Pie de Palo subnetwork (traces are cut and lined up on the *S* arrivals). Theoretical arrival times for *S* and *S*-to-*P* conversions from a 50-km-deep Moho are also shown.

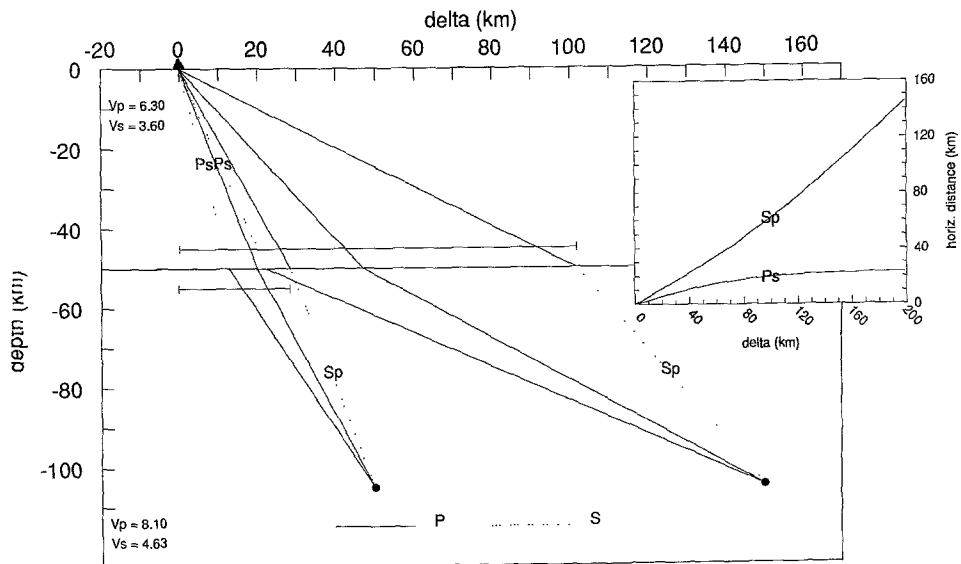


Figure 6. Geometry of ray paths used in this study. Note that the *S*-to-*P* conversion point varies strongly with epicentral distance (see inset).

40-km crustal thickness estimated for the Brazilian craton (Assumpcao and Suarez, 1988) and indicates the crust has undergone a significant amount of crustal thickening, about 12 km, which is a 30% increase. If we assume the brittle activity domain is 30-km thick, as imaged by the crustal seismicity beneath Pie de Palo (Regnier *et al.*, 1992), we can then estimate the ductile lower crust to be 22-km thick, the difference between the Moho depth and the upper crustal thickness. According to Condie (1989), this value for the lower crustal thickness is very close to that for a shield or platform area (19 to 21 km). This would indicate that most crustal thickening occurs through an increase of the brittle domain rather than of the ductile domain of the crust. As pointed out by Sibson (1982), the cutoff depth for microseismicity, identified to the brittle-ductile transition, depends strongly on the geotherm. Here, a moderate to low heat flow, due to the doubling of lithosphere and the absence of volcanic arc (Jordan *et al.*, 1983), associated with an important strain rate, can explain the unusually large thickness of the brittle upper crust.

Precordillera

In order to survey the Moho under the whole network, we have also looked for S_p converted waves at the stations located on the Precordillera. Figure 10 shows a record section of the RZ product for multiple events at the stations of the eastern Precordillera (Figs. 2 and 8).

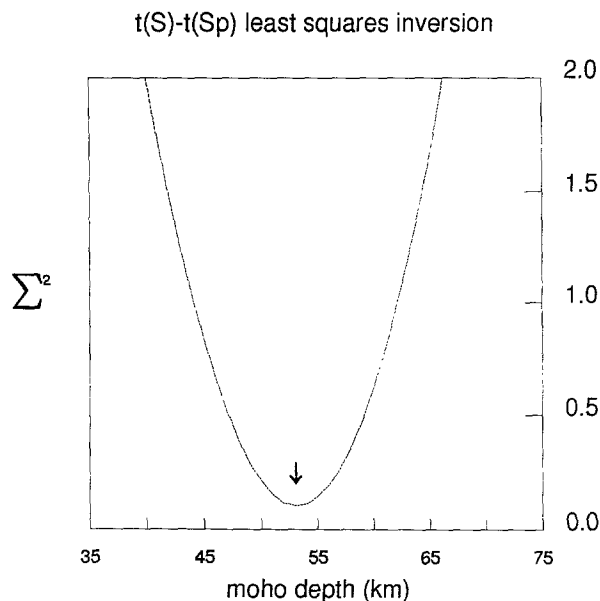


Figure 7. Least-square inversion results to estimate the Moho depth from the relative arrival times $T(S)-T(S_p)$ observed at one station. The rms residuals are plotted against Moho depth for the Bollinger and Langer (1988) crustal velocity model. Source distances are less than 50 km.

It clearly shows arrivals of energy between P and S phases. Large variations in backazimuth together with lateral variation of structure in the crust are probably responsible for the important differences observed in the overall waveform of the S -to- P energy and for the scatter of onset of energy around the computed travel-time curve. Because the energy is split between the radial and tangential component (Fig. 4) for off-azimuth arrivals due to nonplanar or dipping interfaces, the RZ product is not always as large as it would be for a flat layered crust and shows important amplitude variations. A 55-km-deep Moho velocity model has been used to compute the curves shown on Figure 10. Further west, the data recorded at the westernmost stations of the network located on the central Precordillera (Figs. 2 and 8) exhibit very clear S_p phases on the vertical component after low-pass filtering below 3 Hz. Figure 11 shows a multiple events record section of the vertical component at these three stations (i12, o11, and o10). A clear phase is observed throughout the section at about the time of the computed S -to- P converted phase for a 59-km-deep Moho. Traces are lined up on the observed S time and are cut before the S arrival for easier comparison with the product record sections. At very close distances, the S - S_p relative travel time is quite insensitive to earthquake depth, while the S - P time, i.e., the length of plotted signal, shows large variation due to scatter in the depth of the events. The Moho depth found beneath station o09 located between the Sierra Pie de Palo and the eastern Precordillera is 52 km (Fig. 8). This is similar or slightly larger than the average 50-km Moho depth found beneath the southern block of the Sierra Pie de Palo, northeast of station o09. That would indicate that the Moho does not shallow, at least on the west side of the Sierra Pie de Palo, and that the thickening of the crust is continuous from the Sierra Pie de Palo toward the Precordillera. From both the record sections (Figs. 5, 10, and 11) and the Moho depths displayed on Fig. 8, there is a systematic Moho depth increase from east to west. There is about a 3- to 5-km difference in total crustal thickness between the Sierra Pie de Palo and the eastern Precordillera, and there is also a thickness increase between the eastern and the central Precordillera. The distance between the eastern and central Precordillera is about 25 km, which yields an 11° westward sloping Moho for a 5-km depth difference between them. Using this slope estimate, the Moho would be at a 70-km depth beneath the frontal Cordillera if the Moho slope remains constant.

Figure 12 shows the effect of dip on S - S_p relative time. The two curves are for a flat (solid line) and a dipping Moho (dashed line) with a 55-km Moho depth beneath the station (see insert). The time differences between the two curves at distances greater than 120 km are bigger than 1 sec., which is resolvable in the data if such distance dependant variation of the S - S_p time exists. To check whether there is a regional trend or not,

we have mapped S - Sp residual times at all stations on the Precordillera on a single polar plot for a horizontal crust 55- or 60-km thick depending on stations location (Fig. 13). The size of the symbols is proportional to the residual. The residuals for events beneath the stations ($\Delta < 40$ km) are very small, both positive and negative, indicating a good fit of the observed relative travel times to the crustal model. Beyond 40 km, the residuals pattern shows a radial increase of the residual amplitude and an east-west variation of the residual sign similar to the time differences of the dashed curve (dipping Moho) minus the solid curve (flat Moho) from Figure 12. The westward increase of the positive residuals indicates a westward increase of the Moho depth. A 5° to 10° westward slope for the Moho beneath the Precordillera could account for the increase in residual amplitudes.

Discussion

One important result of this study is that the product of orthogonal components to enhance body-wave signal to noise ratio can be a powerful tool, especially when reflected/converted waves are weak and hidden by scattered energy. Synder *et al.* (1990), in processing deep seismic reflection profiles in the same area, came to the

conclusion that the Pampeanas basement has low seismic reflectance. No feature in the lower crust could be identified on their sections. This result is in agreement with the absence of observable P -to- S converted waves from the lower crust in our data. Indeed, P -wave incidence on the Moho from short-distance intermediate-depth earthquakes is generally steep (Fig. 6) for a Ps ray path, and this phase will have significant amplitude only if a high enough velocity contrast is present. Since we seldom found S -wave phases in the P coda of the radial component or large negative pulses on the RZ product (Fig. 4) within the expected time range for Ps phases, the lower crust appears to have low velocity contrast. The very high amplitude of the S wave can, however, generate observable Sp phases (Fig. 4). These qualitative interpretations on the lower crust velocities agree with the velocity model used in this study (Volponi, 1968; Bollinger and Langer, 1988), which comprises a very high lower crust velocity ($V_p = 7.3$ km/sec). For such a crustal velocity model, a low velocity contrast across the Moho discontinuity is likely. We did not model the amplitude of the S -to- P converted arrivals for several reasons. First, body-wave amplitudes are strongly dependent on focal mechanisms and very few focal mechanisms are available for the intermediate-depth events

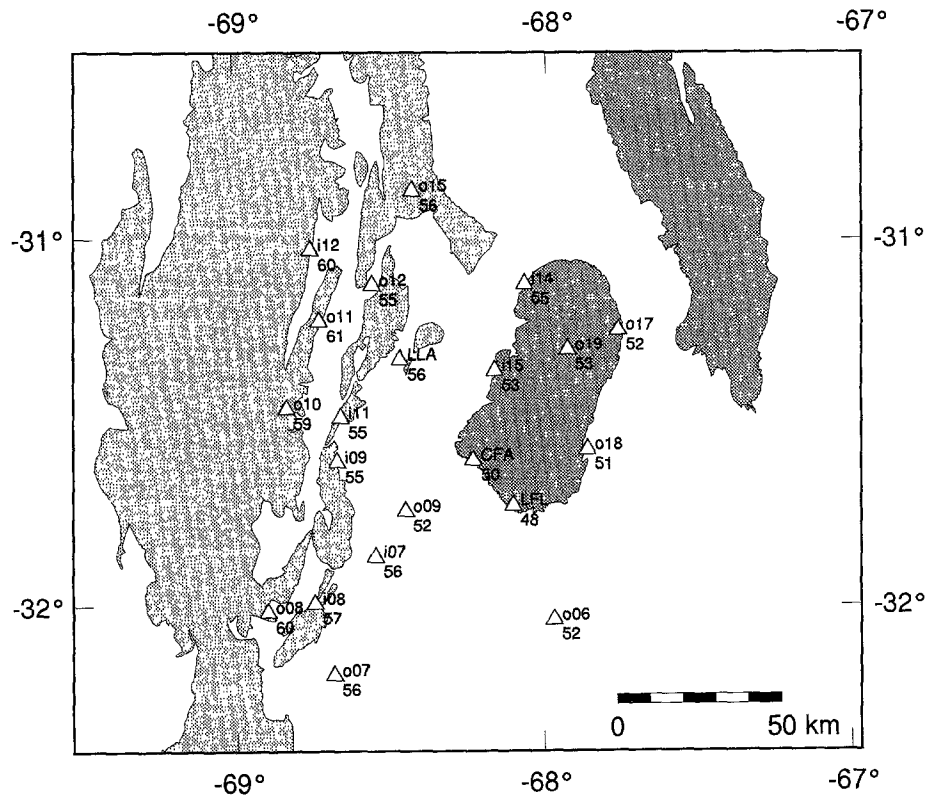


Figure 8. Map of San Juan region showing the Moho depth determined at each individual station. There is a systematic increase of the Moho depth from south to north across the Sierra Pie de Palo. There is also a regional east-west increase of the Moho depth.

(Reta, 1992), making amplitude modeling hazardous. Also, propagation effects such as attenuation, scattering, and focusing/defocusing are obviously present in the short-period data and would prevent successful modeling. It is interesting to note the frequency content variation of the Moho Sp phase as one moves from stations in the eastern to the central Precordillera, as it is probably related to variation of the thickness of the Moho transition zone. The low-frequency Sp phase from beneath the central Precordillera (Fig. 11) would indicate a thinner Moho transition zone than that found under the eastern Precordillera and Sierra Pie de Palo. Alternatively, it can also indicate a larger velocity jump across the Moho.

Our model of crustal thickness variation is summarized in a regional cartoon (Fig. 14) incorporating results of this study with latest tectonic model for the Andean foreland (Regnier *et al.*, 1992; Smalley *et al.*, 1993). The Moho depth determination has been achieved solely with travel-time modeling. The velocity model we used was derived by Volponi (1968) for the lower crust from the refraction method with earthquake data and refined by Bollinger and Langer (1988) for the upper crust from shallow refraction profiles. It is valid for the Sierra Pie de Palo area. Our Moho study implicitly makes the assumption that crustal velocities do not vary much from

the Sierra Pie de Palo to the Precordillera since detailed velocity models for both areas are unavailable. Because there is a trade-off between crustal thicknesses and velocities in crustal structure determination, the increase of the S - Sp time from east to west could be also explained by an east-west decrease of the mean crustal velocity instead of an east-west increase of the crustal thickness. However, it is interesting to note that the crustal seismicity is also deepening westward, with maximum depth ranging from 30 km beneath the Sierra Pie de Palo (Regnier *et al.*, 1992) to between 35 and 40 km beneath the eastern Precordillera (Smalley *et al.*, 1993). Both maximum depth values were obtained through independent JHD locations, which correct for lateral crustal structure variations (Pujol *et al.*, 1991). Between the Sierra Pie de Palo and the eastern Precordillera, the increase of the Moho depth is equivalent to the deepening of the seismicity, ca. 5 km, indicating that both the Moho and the upper crust lower boundary show the same westward slope. This similar behavior of both boundaries strongly suggests an east-west crustal thickness variation as a major component of the S - Sp times increase; the amount of lateral variation of velocity cannot be constrained by our data. An important consequence of our model (Fig. 14) is that, along the same east-west profile, the ductile lower crust shows no thickness variation and remains 21-km

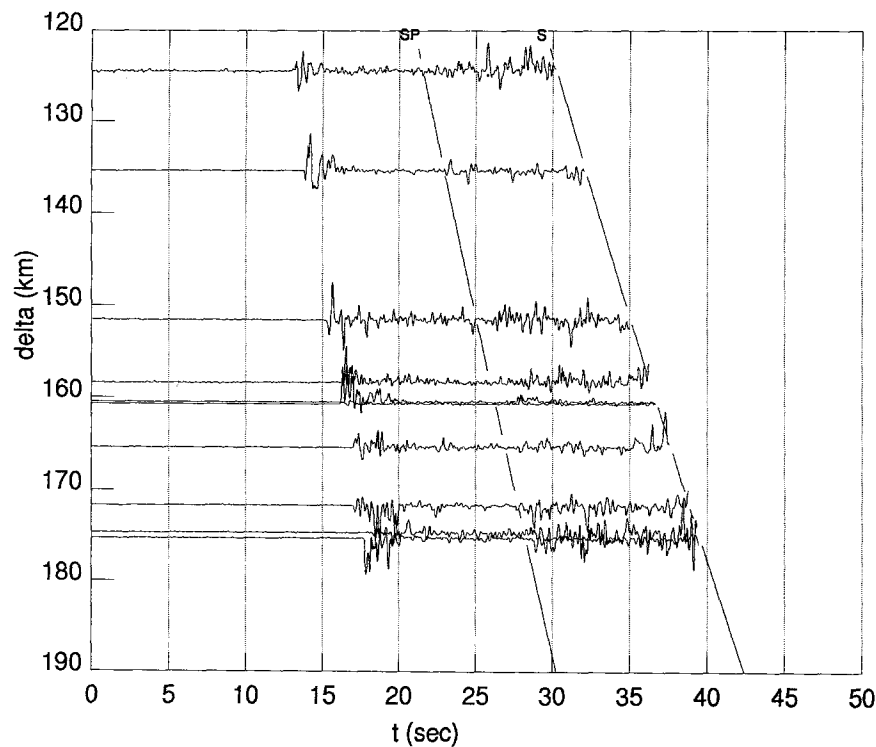


Figure 9. Record section at Precordillera stations of RZ product from intermediate-depth earthquakes beneath the Sierras Pampeanas province. Delta is large enough so the S -to- P conversion points lay beneath the Sierra Pie de Palo (Fig. 6). The 50-km Moho depth estimated from this record section is in agreement with the Moho depth determinations at the single station on Sierra Pie de Palo.

thick, sloping 5° to 10° westward. The crustal thickening occurs through an increase of the brittle upper crust beneath both the Pampean foreland and the Precordillera. Although the two areas have different seismicity patterns, partly controlled by the different time periods elapsed since their last respective large or characteristic event (1944 for the Precordillera and 1977 for the Sierra Pie de Palo), they probably have comparable crustal rheology. The deepening of both the ductile lower crust and the seismicity suggests that the Pampean crust is underthrusting beneath the Precordillera. The east-west increase of the depth to the basement also supports this model. The depth to the Precambrian basement is variable in the foreland basin west of the Sierra Pie de Palo (Tulum valley, Fig. 2), but no deeper than 5 km (Bollinger and Langer, 1988). Westward, the depth to the décollement thickens from 9 km beneath the eastern Pre-

cordillera to about 15 km beneath the central Precordillera (Allmendinger *et al.*, 1990). The increase of the depth to the basement is then of the same order as the Moho depth increase and also suggests the foreland crust underthrusts beneath the Precordilleran thin-skinned belt.

As pointed out by Allmendinger *et al.* (1990), crustal scale balanced sections are very powerful in this segment of the Andes for two major reasons: (1) the absence of important magmatic addition to the andean crust during the last ~ 9 m.y. (Kay *et al.*, 1988) and (2) the boundary conditions, both horizontally and vertically, set up by the subducted plate, which severely limit the domain of deformation of the South American lithosphere above the Nazca plate. Finally, the geometry of the plate convergence and the topography of the Andes do not show evidence of indentation and of large lateral motion of lithospheric blocks (Isacks, 1988), which allows us to

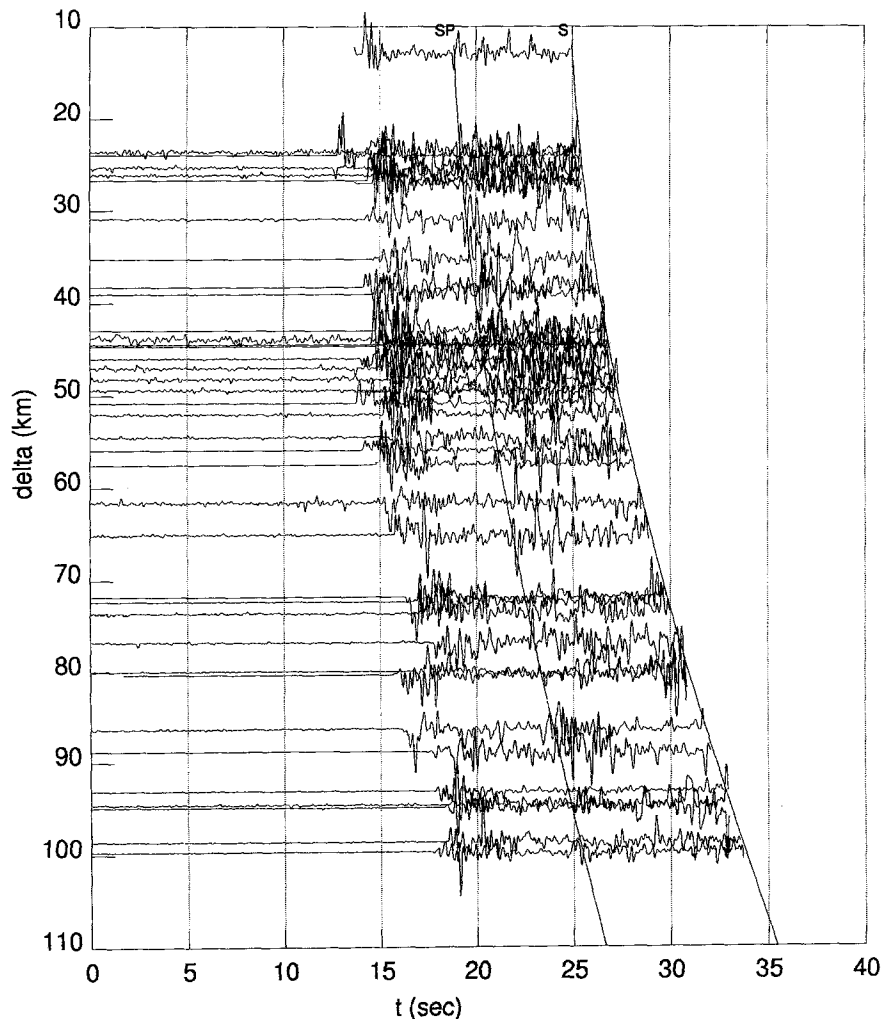


Figure 10. Multiple events RZ product record section at stations of the eastern Precordillera (o15, o12, LLA, i11, i09, i07, i08, and o07). A major arrival of energy is observed between the P and S phases throughout the section at about the time of the computed S-to-P converted phase for a 55-km-deep Moho. As in Figure 5, traces are cut at the S arrival.

assume a 1D shortening across the orogen. Although it is very likely that a 3D distribution of deformation occurs often locally, the 1D shortening model is probably valid on a regional scale. If this assumption is not true, this would lead to an underestimate of the actual shortening across the orogen when computed from thickening inferred in a single cross section of the Andes only.

We estimated, using area balancing, the shortening of the Sierras Pampeanas province for the last 5 to 10 m.y., during which compressive forces caused thick-skinned deformation (Camino, 1979). The actual east-west width of the Sierras Pampeanas province is about 5° (Jordan and Allmendinger, 1986), which is 481 km at the latitude 30° south. We estimated in this study the crustal thickness to be 52 km at the western margin of the province and we assumed the original thickness was 40 km. The initial width was then 625 km to match the same area after deformation. The total shortening is 141 km or 29%. This value must be seen as the upper bound for the shortening since we assumed a uniform crustal

thickening all over the Sierras Pampeanas province. If we assume a progressive linear thickening from east to west, starting with a 40-km-thick crust along the eastern margin (i.e., no thickening), the initial width becomes 553 km and the total shortening 72 km or 15% (Fig. 15). A periodic crustal thickening with maxima beneath each individual range would give about the same amount of total shortening as the ramp model. These shortening values are much larger than the 2 to 4% estimate of Jordan and Allmendinger (1986) based on cumulative shortening across the entire Sierras Pampeanas fault system. Snyder *et al.* (1990) suggested, from interpretation of deep seismic sounding across Pampeanas fault systems, that Jordan and Allmendinger's estimate might be too low. However, the important discrepancy between the different estimates could indicate that crustal thickening cannot be explained by horizontal compression alone and requires addition of magmas in the lower crust by underplating or crustal intrusion. Both a positive density anomaly (Introcaso, 1980) and a high compressional wave

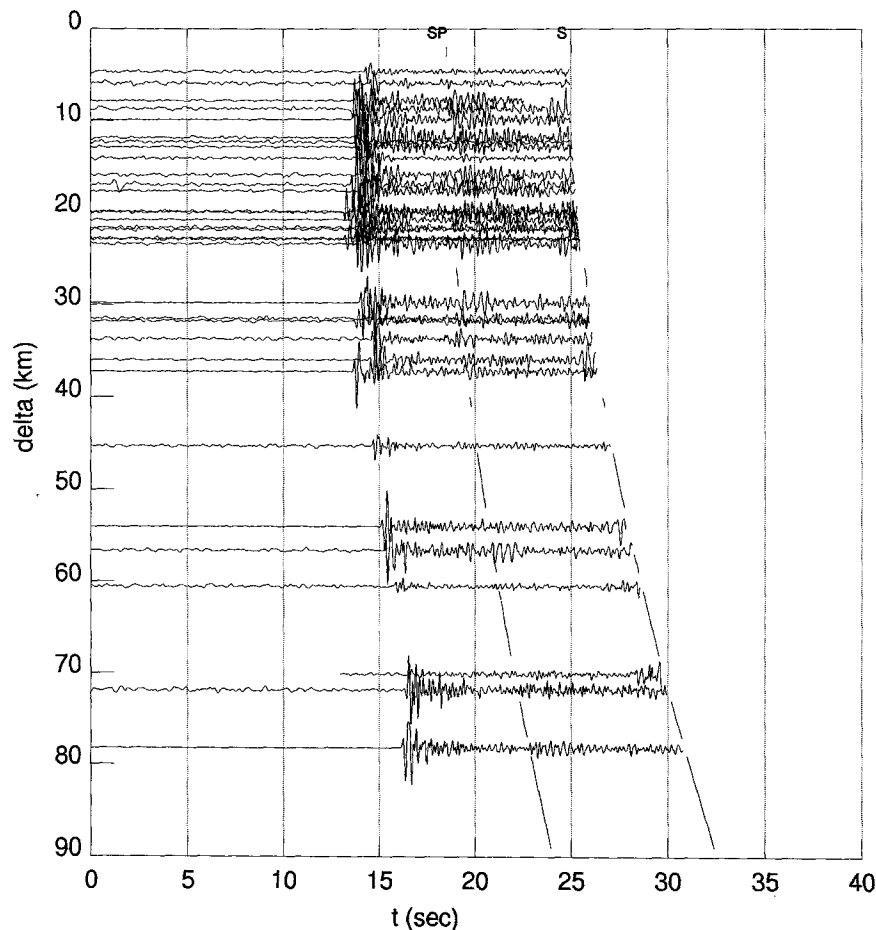


Figure 11. Multiple events record section of the vertical component at stations on the central Precordillera (i12, o11, and o10). The seismograms are low-pass filtered below 3 Hz. A clear compressional phase is observed throughout the section at the time of the *S*-to-*P* converted phase for a 59-km-deep Moho. Traces are lined up on the observed *S* time and are cut before the *S* arrival.

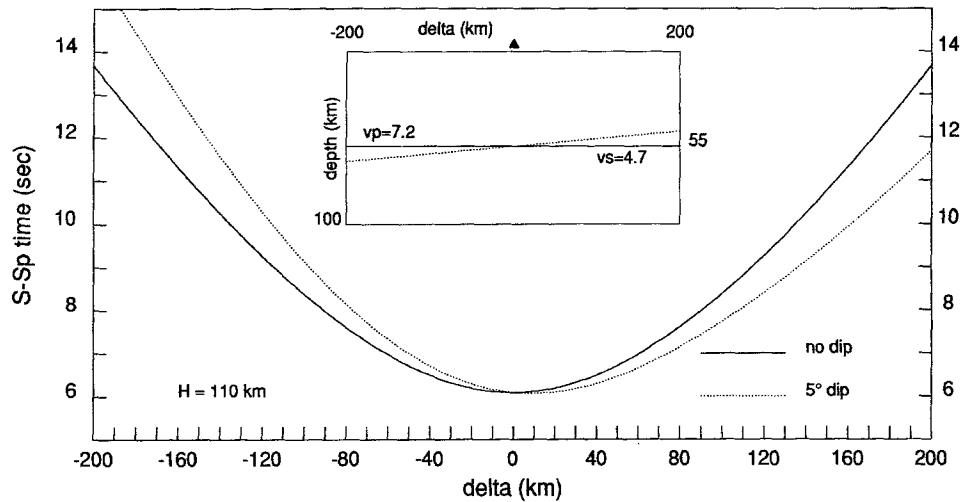


Figure 12. Computed *S-Sp* relative travel time as a function of the epicentral distance for a flat (solid curve) and a 5° dipping (dashed curve) Moho. The inset shows the crustal model used for the computation. Note the large time differences between the two curves at distances greater than 100 km and their opposite sign on both sides of the station.

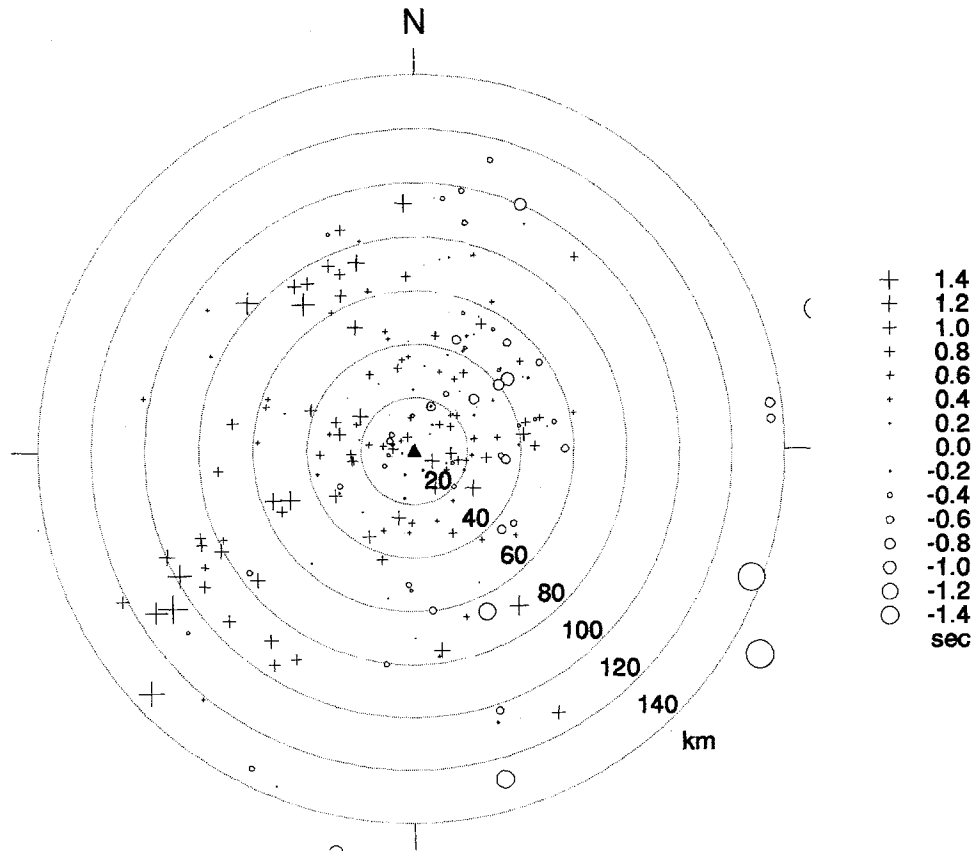


Figure 13. Polar plot of the *S-Sp* residual times at all Precordillera stations for a horizontal crust 55- or 60-km thick depending on station location (eastern or central Precordillera). The size of the symbols is proportional to the residual. A plus is a positive residual and an open circle a negative residual. The triangle shows the station location. The increase of the residual amplitudes away from the station and the distribution of positive and negative residuals indicate that the Moho is dipping westward beneath the Precordillera.

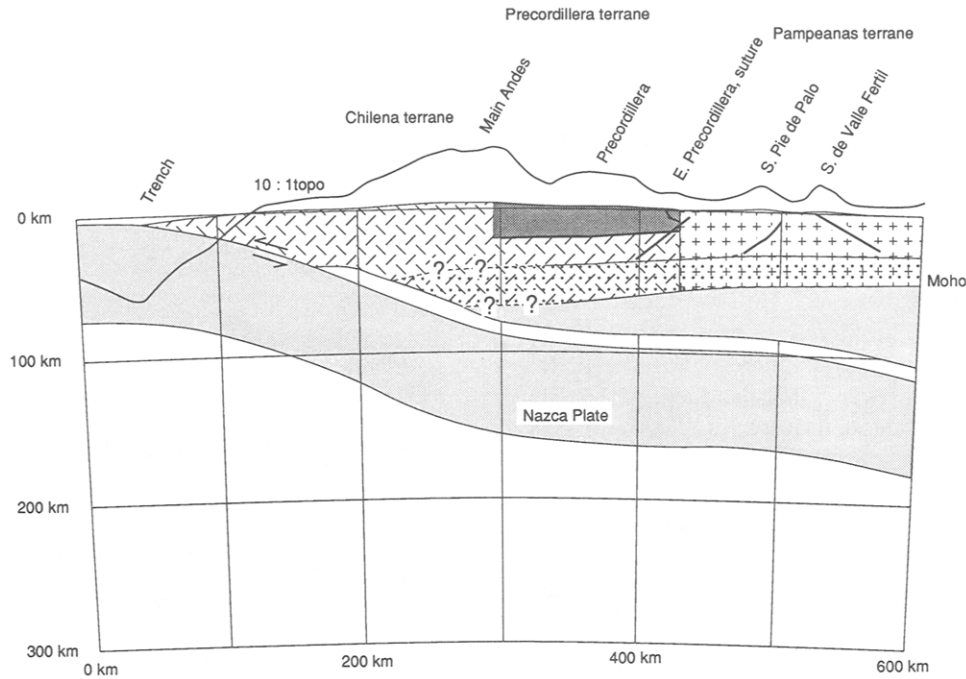


Figure 14. Regional cartoon incorporating results of this study (Moho depth and ductile layer thickness). The crossed area is the Sierra Pampeanas province; dashed area, Main Andes and Chilena terrane; dark grey area, Precordillera thin-skinned tectonic province; light grey area, lithosphere. The dotted strip on top of the Sierras Pampeanas and Main Andes province represents the ductile deformation zone.

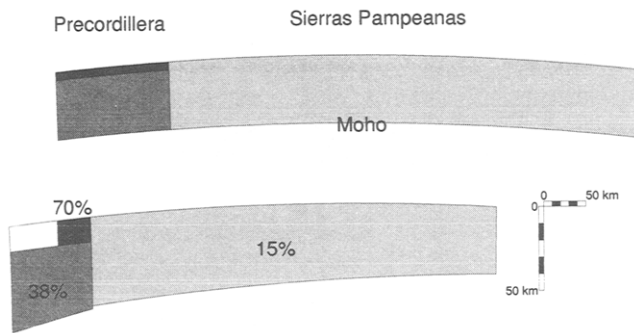


Figure 15. Schematic cross section of the Precordillera and Sierras Pampeanas terranes before (top) and after (bottom) shortening. The shortening values are indicated for each unit. The Moho slope is 5° in the Precordillera province. The vertical exaggeration is ×2.

velocity (Volponi, 1968) in the lower crust support the model of underplated mafic magmas in the Pampean crust. Thus, the thickening of the Pampean crust is due to the combination of addition of mafic magmas and horizontal compressive forces acting on the South American lithosphere. Without detailed information on the lower crust layering, the respective importance of both causes is difficult to establish. The *S_p* coda (Figs. 4 and 10) usually shows that the lower crust is layered and large ampli-

tudes are present, indicating wave conversions at higher velocity contrasts than the Moho discontinuity. These velocity contrasts could represent the transitions from underplated magmas to standard ductile lower crust.

The shortening across the Precordillera has been estimated by Allmendinger *et al.* (1990) to 95 km or 70%, with an original 135-km-wide belt. Using straightforward area balancing techniques on the whole crust, this amount of shortening, together with an initial 40-km-thick crust, gives an estimate of the present crustal thickness that is totally unrealistic (>100 km). The uncoupling of the domains above and below the décollement provides a simple way to accommodate different deformation rates for the two domains. Before shortening, the thickness of the crustal domain below the décollement was about 35 km, assuming the original sedimentary wedge was 5-km thick (Allmendinger *et al.*, 1990) and the crust 40-km thick. The present depth to the décollement is estimated to be 15 km by Allmendinger *et al.* (1990) with seismic reflection data. Together with the crustal thicknesses found in this study, that leads to thicknesses of 40 and 45 km for the crust below the décollement for the eastern and central Precordillera, respectively. Assuming an original width of 135 km and a 10° westward Moho slope, the actual width of the domain below the décollement should be 86 km to match the same area after deformation. That is a total short-

ening for the crust below the décollement of 49 km or 57%. A 5° Moho slope would give a present width of 97.4 km, a shortening of 37 km or 38% (Fig. 15). In these models, the Moho at the western boundary of the Precordillera lower crust is at a depth of 70.16 km and 63.52 km for a 10° and 5° Moho slope, respectively. This model also implies the Precordillera lower crust and the décollement should now extend beneath the principal mountain belts westward of the westernmost limit of the Precordillera (Figs. 14 and 15). No lower crustal velocity is known beneath the Precordillera, so the presence of underplated mafic magmas cannot be discussed. It is likely, as one goes westward, that the ductile thickening becomes more important as in Isacks' (1988) shortening model.

Conclusions

Analysis of converted wave travel times from intermediate-depth local earthquakes in the Sierras Pampeanas and Precordillera provinces clearly shows a continuous east–west deepening of the Moho from 50 to 60 km, respectively, which we interpret as the underthrusting of the South American craton beneath the Andean mountain belts. A 5° to 10° westward dip of the Moho under the Andean foreland is estimated. Thickening inferred from measured crustal thickness suggests that the Pampean foreland crust has undergone a 30% increase, or about 12 km, during the last 10 m.y. In the central Precordillera, the crust below the décollement also has thickened by 10 km. In both areas of the foreland, most of the crustal thickening resulted in a thickness increase of the brittle upper crust imaged by unusually deep crustal seismicity, while the ductile lower crust shows no significant thickness variation with respect to that of stable continental crust. This rheological behavior of the crust is likely due to an increase in strain rate and to thermal effects linked to the presence of an horizontal slab beneath the Andean foreland. The shortening across the Sierras Pampeanas is estimated to be around 15% for a model in which crustal thickness variation is due to horizontal compression only, but could be slightly less depending of the amount of magma addition in the lower crust. The shortening across the Precordillera province would change from 70% in the sediments of the thin-skinned thrust belt above the décollement to at least 38% below the décollement where basement involved deformations are present.

Acknowledgments

We would like to thank J. C. Castano, R. Recio, and N. Puebla of the Instituto Nacional de Prevención Sísmica (INPRES) in San Juan, Argentina, and J. Pujol (CERI) for their scientific and logistical support. We depended greatly on our engineer G. Steiner (CERI), technicians J. Bollwerk (CERI), and F. Bondoux (ORSTOM), and field crew members J.-L. Chatelain (ORSTOM), J. Vlasity (CERI), D. Vlasity

(CERI), T. Cahill (Cornell), C. Avila (INPRES), and M. C. Reta (INPRES). We thank John Butcher for draftings figures. This work was supported by the Institut Français de Recherche Scientifique pour le Développement en Coopération (ORSTOM), National Science Foundation Grant Numbers EAR-8608301 and EAR-8804925, and the State of Tennessee Centers of Excellence Program.

References

- Allmendinger, R., D. Figueroa, E. Snyder, J. Beer, C. Mpodozis, and B. L. Isacks (1990). Foreland shortening and crustal balancing in the Andes at 30° latitude, *Tectonics* **9**, 789–809.
- Assumpcao, M. and G. Suarez (1988). Source mechanisms of moderate-size earthquakes and stress orientation in mid-plate South America, *Geophys. J.* **92**, 253–267.
- Bath, M. and R. Stefansson (1966). S-P conversion at the base of the crust, *Ann. Geofis.* **19**, 119–130.
- Bastias, H. E., N. E. Weidmann, and A. P. Pérez (1984). Dos zonas de fallamiento Pliocuaternario en la Precordillera de San Juan, in *IX Cong. Geol. Argentino*, Vol. 2, 329–341.
- Bollinger, G. A. and C. J. Langer (1988). Development of a velocity model for locating aftershocks in the Sierra Pie de Palo region of western Argentina, *U.S. Geol. Surv. Bull.*, 1795.
- Caminos, R. (1979). Cordillera frontal, in *Segundo Simposio de Geología Regional Argentina*, Acad. Nac. Ciencias, Córdoba, 397–454.
- Caminos, R., C. A. Cingolani, and F. Hervé (1982). Eastern Linares, Geochronology of the pre Andean metamorphism and magmatism in the Andean Cordillera between latitudes 30° and 36°S, *Earth Sci. Rev.* **18**, 253–283.
- Chiu, J. M., B. L. Isacks, and R. K. Cardwell (1986). Studies of crustal converted waves using short period seismograms recorded in the Vanuatu Island arc, *Bull. Seism. Soc. Am.* **76**, 177–199.
- Chiu, J. M., G. C. Steiner, R. Smalley, Jr., and A. C. Johnston (1991). The PANDA seismic array—a simple, working system, *Bull. Seism. Soc. Am.* **81**, no. 3, 1000–1014.
- Condie, K. C. (1989). *Plate Tectonics and Crustal Evolution*, Pergamon Press Inc., Maxwell House, Fairview Park, Elmsford, New York.
- Dickenson, W. R. and W. S. Snyder (1978). Plate tectonics of the Laramide Orogeny, Laramide folding associated with basement block faulting in the western United States, *Mem. Geol. Soc. Am. Num.* **151**, V. Matthews III (Editor), 355–366.
- Frohlich, C. (1979). An efficient method for joint hypocenter determination for large groups of earthquakes, *Computers Geosci.* **5**, 387–389.
- INPRES (Instituto Nacional de Prevención Sísmica) (1977). El terremoto de San Juan del 23 de Noviembre de 1977, Informe Preliminar, Republica Argentina, San Juan, 103 pp.
- Introcaso, A. (1980). Resultados gravimétricos en la banda latitudinal de Argentina central y países vecinos, *Rev. Geofis., Inst. Panam. de Geogr. Hist.* **12**, 5–25.
- Isacks, B. L. (1988). Uplift of the central Andean Plateau and bending of the Bolivian Orocline, *J. Geophys. Res.* **93**, 3211–3231.
- Jacob, A. W. B. and D. C. Booth (1977). Observation of PS reflections from the Moho, *J. Geophys. Res.* **43**, 687–692.
- Johnsson, P. A., A. Johnson, N. M. Jordan, and C. W. Naeser (1984). Magnetic polarity stratigraphy and age of the Quebrada del Cura, Rio Jachal, and Mogna Formations near Huaco, San Juan province, Argentina, in *IX Cong. Geol. Argentino*, Vol. 3, 81–96.
- Jordan, T. H. and L. N. Frazer (1975). Crustal and upper mantle structure from Sp phases, *J. Geophys. Res.* **80**, no. B11, 1504–1518.
- Jordan, T. E., B. Isacks, R. Allmendinger, J. Brewer, V. Ramos,

- and C. Ando (1983). Andean tectonics related to geometry of subducted Nazca plate, *Geol. Soc. Am. Bull.* **94**, 341–361.
- Jordan, T. E. and R. W. Allmendinger (1986). The Sierras Pampeanas of Argentina: a modern analogue of Rocky Mountain foreland deformation. *Amer. J. Sci.* **286**, 737–764.
- Kadinsky-Cade, K. and R. Reilinger (1985). Surface deformation associated with the November 23, 1977, Caucete, Argentina earthquake sequence, *J. Geophys. Res.* **90**, no. B14, 12691–12700.
- Kay, S. M., V. Maksae, R. Moscoso, C. Mpodozis, C. Nasi, and C. E. Gordillo (1988). Tertiary Andean magmatism in Chile and Argentina between 28°S and 33°S: correlation of magmatic chemistry with a changing Benioff zone, *J. S. Am. Earth Sci.* **1**, 21–38.
- Klein, F. W. (1978). Hypocenter location program HYPOINVERSE, part 1, users guide to versions 1, 2, 3, and 4, *U.S. Geol. Surv. Open-File Rept.* 78-694.
- Langston, C. A. (1977). The effect of planar dipping structure on source and receiver responses for constant ray parameter, *Bull. Seism. Soc. Am.* **67**, 1029–1050.
- Langston, C. A. (1979). Structure under Mount Rainier, Washington, inferred from teleseismic body waves, *J. Geophys. Res.* **84**, 4749–4762.
- Li, Y., C. H. Thurber, and C. G. Munson (1992). Profile of discontinuities beneath Hawaii from S to P converted seismic waves, *Geophys. Res. Lett.* **19**, no. 2, 111–114.
- Pujol, J., J.-M. Chiu, R. Smalley, Jr., M. Regnier, B. L. Isacks, J.-L. Chatelain, J. Vlasity, D. Vlasity, J. C. Castano, and N. Puebla (1991). Lateral velocity variations in the Andean foreland in Argentina determined with the JHD method, *Bull. Seism. Soc. Am.* **81**, no. 6, 2441–2457.
- Regnier, M., J.-L. Chatelain, R. Smalley, Jr., J.-M. Chiu, B. L. Isacks, M. Araujo (1992). Seismotectonics of the Sierra Pie de Palo, a basement block uplift in the Andean foreland, Argentina, *Bull. Seism. Soc. Am.* **82**, no. 6.
- Reta, M. C. (1992). High resolution view of the Wadati-Benioff zone and determination of the Moho depth in San Juan, Argentina, *M. S. Thesis*, Memphis State University, Memphis Tennessee.
- Sheffels, B. M. (1990). Lower bound on the amount of crustal shortening in the central Bolivian Andes, *Geology* **18**, 812–815.
- Sibson, R. H. (1982). Fault zone models, heat flow, and the depth distribution of earthquakes in the continental crust of the United States, *Bull. Seism. Soc. Am.* **72**, no. 1, 151–163.
- Smalley, R., Jr. and B. L. Isacks (1990). Seismotectonics of thin and thick-skinned deformation in the Andean foreland from local network data: evidence for a seismogenic lower crust, *J. Geophys. Res.* **95**, no. B8, 12487–112498.
- Smalley, R., J. Pujol, M. Regnier, J. M. Chiu, B. L. Isacks, M. Araujo, and N. Puebla (1993). Basement seismicity beneath the Andean Precordillera thin-skinned thrust belt and its implications for crustal and lithospheric behavior, *Tectonics* **12**, no. 1, 63–76.
- Smith, W. D. (1970). S to P conversion as an aid to crustal studies. *Geophys. J. R. Astr. Soc.* **19**, 513–519.
- Snyder, D. B., V. A. Ramos, and R. W. Allmendinger (1990). Thick-skinned deformation observed on deep seismic reflection profiles in Western Argentina, *Tectonics* **9**, no. 4, 773–788.
- Vlasity, D. (1988). A crustal seismicity study in the San Juan, Argentina region using digital seismograms collected by the Panda Array, *M.S. Thesis*, Memphis State University, Memphis, Tennessee.
- Volponi, F. S. (1968). Los terremotos de Mendoza del 21 de Octubre de 1968 y la estructura de la corteza terrestre, in *Acta Cuyana de Ingeniería*, Vol. XII, Instituto Sismológico Zonda, Facultad de Ingeniería, Universidad Nacional de Cuyo, San Juan, Argentina, 95–110.
- Whitney, R. A., H. E. Bastias, and D. B. Slemmons (1984). Thrust fault near-surface geometry and age of the last displacement determined from geographic and trench data in the Precordillera of San Juan province, Argentina (abstract), *Geol. Soc. Am.* **16**, 693.
- Institut Français de Recherche Scientifique
pour le Développement en Coopération (ORSTOM)
BP A5 Noumea Cedex
New Caledonia, South West Pacific
(M.R.)
- Center for Earthquake Research and Information (CERI)
Memphis State University
Memphis, Tennessee
(J.-M.C., R.S.J.)
- Institute for the Study of the Continents (INSTOC)
Cornell University
Ithaca, New York
(B.L.I.)
- Intituto Nacional de Prevención Sísmica (INPRES)
(M.A.)